Chemical Geology xxx (xxxx) xxx–xxx

Contents lists available at ScienceDirect

Chemical Geology

journal homepage: www.elsevier.com/locate/chemgeo

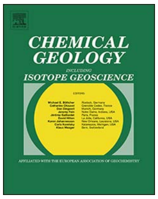

Pb isotopes in the impact melt breccia 66095: Association with the Imbrium basin and the isotopic composition of lithologies at the Apollo 16 landing site

Joshua F. Snape[a,*], Alexander A. Nemchin[a,b], Jeremy J. Bellucci[a], Martin J. Whitehouse[a]

[a] Department of Geosciences, Swedish Museum of Natural History, SE-104 05 Stockholm, Sweden.
[b] Department of Applied Geology, Curtin University, Perth, WA 6845, Australia.

ARTICLE INFO

Keywords:
Lunar Pb
Pb isotopes
66095
Imbrium
Initial Pb

ABSTRACT

Recent in situ Secondary Ion Mass Spectrometry (SIMS) Pb isotope analyses of lunar basalts have provided precise crystallisation ages and initial Pb isotopic compositions for these samples. In this study, the same approach has been tested in the Apollo 16 impact melt breccia 66095, referred to as the "Rusty Rock" due to its enrichments in volatile elements, including Pb. Based on these analyses of the breccia, a Pb-Pb isochron age of 3909 ± 17 Ma (at the 95% confidence level) and an initial Pb composition for 66095 have been determined. This age is interpreted as representing the time of breccia formation that, when combined with recent studies of lunar breccias, can be linked to the Imbrium basin forming impact. The directly measured initial Pb composition of the breccia from this work is similar a modelled compositions presented previously, and likely reflects an average value for the lithologies present at the Apollo 16 landing site at the time that the Imbrium ejecta was emplaced. The 66095 initial Pb isotopic composition is compared with the compositions in other lunar samples and the nature of the endmember lithologies in this mixture has been discussed within the framework of a multiple stage model of Pb isotope evolution on the Moon. This study demonstrates the effectiveness of this technique beyond its application in crystalline basalts, opening up the possibility of obtaining precise geochronological and Pb isotopic compositions from a broader sample set than was previously recognised.

1. Introduction

The Pb isotope compositions of lunar samples indicate that μ-values (the ratio of $^{238}U/^{204}Pb$ extrapolated to the present) in many lunar lithologies and their mantle sources are significantly higher (~100–600; Tatsumoto, 1970; Tera and Wasserburg, 1974; Gaffney et al., 2007a; Nemchin et al., 2011; Snape et al., 2016a) than those determined for the Earth (terrestrial mantle μ-values typically being ~8–10; Kramers and Tolstikhin, 1997) and other planetary bodies (e.g. Mars with mantle μ-values of ~1–5; Gaffney et al., 2007b; Bellucci et al., 2015). Despite evidence of low-μ lunar mantle sources identified in several samples (e.g. Hanan and Tilton, 1987; Misawa et al., 1993; Torigoye-Kita et al., 1995; Premo et al., 1999), the generally high-μ values determined for most lunar silicate reservoirs suggest a profound depletion of Pb in the Moon compared to the Earth, which has previously been attributed to early volatile loss (e.g. Tatsumoto, 1970), potentially during the formation of the Moon during a giant impact between the proto-Earth and another planetary body (Hartmann and Davis, 1975). As a consequence of the low Pb abundance in samples from the Moon, efforts to measure the isotopic composition of initial lunar Pb are typically hindered by the increased susceptibility to terrestrial contamination (Gaffney et al., 2007a; Nemchin et al., 2011). In addition, the highly radiogenic nature of lunar Pb isotope compositions makes it difficult to distinguish between Pb generated by in situ radiogenic decay of U after the rocks were formed and lunar initial Pb inherited from the source(s) of the samples during their formation (e.g. Nemchin et al., 2011).

Recent work by Snape et al. (2016a) interpreted the Pb isotopic compositions measured in six lunar basalts as representing a combination of three main constituents: (1) initial Pb introduced to the samples when they crystallised, (2) radiogenic Pb formed by the decay of U in the sample after the introduction of the initial Pb, and (3) terrestrial contamination. For each sample, these three constituents define a triangular array of points on a plot of $^{207}Pb/^{206}Pb$ versus $^{204}Pb/^{206}Pb$ (Fig. 1), in which the analyses with the highest $^{204}Pb/^{206}Pb$ trend towards terrestrial Pb isotope compositions (Stacey and Kramers, 1975). The addition of primitive meteoritic Pb would result in pulling the measured compositions towards the right side of this plot (Fig. 1),

---

* Corresponding author.
E-mail address: joshua.snape@nrm.se (J.F. Snape).

http://dx.doi.org/10.1016/j.chemgeo.2017.07.012
Received 9 March 2017; Received in revised form 11 July 2017; Accepted 13 July 2017

Please cite this article as: Snape, J.F., Chemical Geology (2017), http://dx.doi.org/10.1016/j.chemgeo.2017.07.012

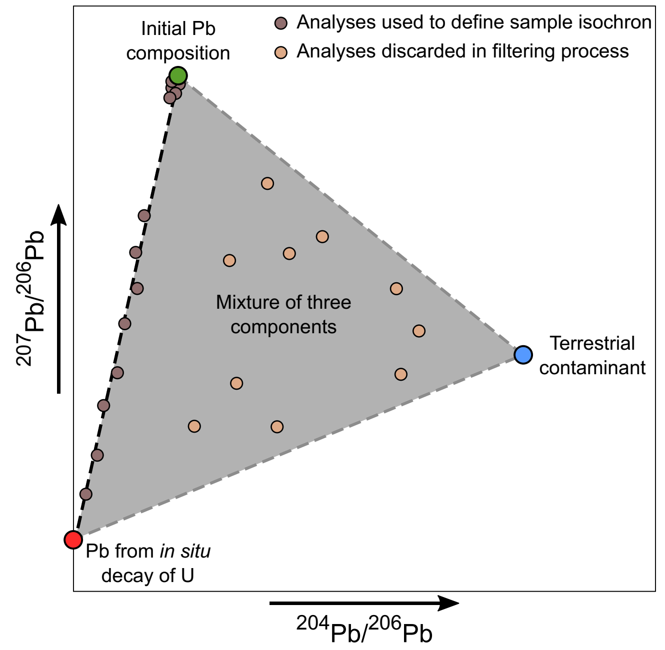

Fig. 1. Schematic illustration of the three component mixture of Pb isotope compositions when plotted as $^{207}\text{Pb}/^{206}\text{Pb}$ versus $^{204}\text{Pb}/^{206}\text{Pb}$. Figure adapted from Snape et al. (2016a).

although this effect appears to be negligible in the samples analysed to date (Snape et al., 2016a). The data along the bounding edge on the left side of the triangle form an isochron defining the time when the sample crystallised, the variability in compositions along this line reflecting the different μ-values of the individual minerals. The analyses falling on this isochron with the highest $^{207}\text{Pb}/^{206}\text{Pb}$ ratios represent the best estimate for the initial Pb component that was incorporated into the rocks when they crystallised, while the analyses with the lowest $^{207}\text{Pb}/^{206}\text{Pb}$ ratios contain the maximum amount of the in situ radiogenic Pb component. Any analyses falling at intermediate locations between the apices of the triangle are interpreted as representing mixtures of these three endmember compositions. This approach was used to determine precise crystallisation ages for these basalts that correlated with previously published values (Snape et al., 2016a and references therein). In crystalline basalt samples, the existence of a well-defined initial Pb composition and a more radiogenic endmember resulting from the in situ decay of U is a logical consequence of how these samples formed. This study aims to test the applicability of this approach to non-basaltic lunar samples by investigating the Pb isotopic compositions of mineral phases in the Apollo 16 polymict impact melt breccia 66095, where a single well-defined initial Pb composition (and the resulting mixing relationship described above) would not necessarily be inevitable or expected.

There are two main reasons for testing this analytical approach in 66095, the first of which being the textural and petrologic nature of the sample. Previous studies describe 66095 as a clast-rich impact melt breccia with a subophitic to ophitic matrix making up about 80% of the rock (Bass, 1972; Garrison and Taylor, 1980; Ryder and Norman, 1980). The Pb isotope compositions of phases in the crystalline melt matrix of the breccia can theoretically be treated in a similar manner to crystalline basalts, with the exception that the initial Pb component identified will represent a homogenised mixture of Pb that was mobilised in the impact melt, and the Pb-Pb isochron age will relate to the crystallisation of that impact melt.

The second reason for studying 66095 is that it exhibits a notable enrichment (relative to other lunar samples) in volatile elements, such as Cl, Zn and Pb (e.g. Krahenbuhl et al., 1973; El Goresy et al., 1973). Enrichments in volatiles were identified in other Apollo 16 breccias, but 66095 stands out as having the highest abundances of such elements (Krahenbuhl et al., 1973). Furthermore, it appears that a significant amount of the Pb in the sample is not supported by the presence of U and cannot be explained by in situ radiogenic decay since the formation of the breccia, but instead represents an initial Pb component incorporated into the breccia (Nunes and Tatsumoto, 1973; El Goresy et al., 1973). The volatile enrichments in the 66095 were previously identified as being associated with the akaganéite (a hydrated iron oxide; FeOOH) "rust" that is a characteristic feature of the breccia (Bass, 1972; Taylor et al., 1974), with Pb being concentrated at the boundaries between akaganéite and troilite (El Goresy et al., 1973). In order to assess the validity of the Pb-Pb isochron approach in 66095, it will be necessary to establish whether the Pb was introduced to the sample as part of the breccia formation process or at a significantly later time.

2. Material and methods

2.1. Sample descriptions

Four sections of 66095 were analysed in this study (66095,77; 66095,85; 66095,222; 66095,322). Three of the sections (77; 222; 322) consist almost entirely of the subophitic to ophitic impact melt texture that makes up the breccia matrix. The melt matrix is characterised by plagioclase forming subhedral plagioclase laths between ~0.01–0.07 mm in length and occasional larger (~0.1–0.3 mm) subhedral to anhedral grains, partially enclosed in pyroxene (Fig. 2). This is consistent with previous studies of the breccia which described the matrix as containing plagioclase (50–60% by mode), pigeonite (up to 30%) and olivine (up to 10%), with accessory phases including cohenite, ilmenite, FeNi metal with intergrowths of schreibersite, as well as assemblages of troilite and sphalerite (Bass, 1972; El Goresy et al., 1973; Taylor et al., 1974; Garrison and Taylor, 1980). Highland "basalt" clasts previously identified in 66095 have been interpreted as

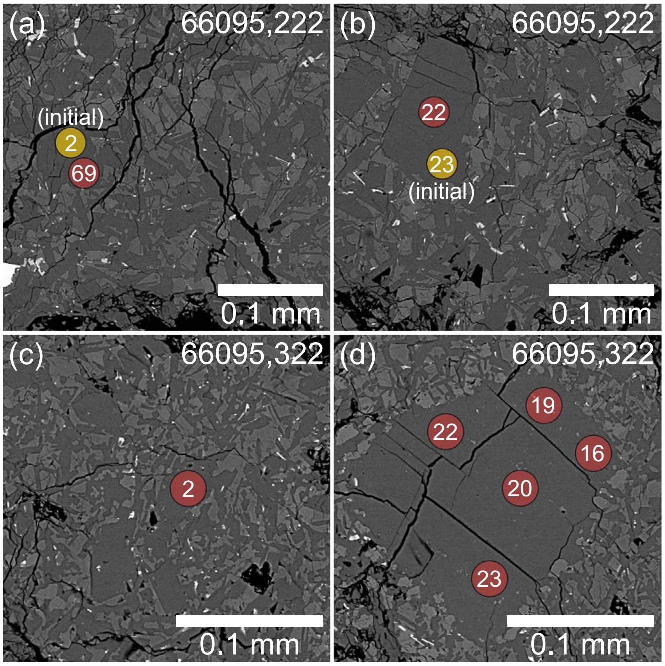

Fig. 2. Back Scattered Electron (BSE) images showing the crystalline melt matrix textures in the 66095,222 and 66095,322 sections. Also indicated are the locations of several SIMS analyses that were used to construct the Pb-Pb isochron for the sample, including two points (indicated with yellow spots) that were used to calculate the initial Pb composition. The numbers in the SIMS spots correspond to the analysis numbers that are included in Supplementary Table B.1. (For interpretation of the references to colour in this figure legend, the reader is referred to the web version of this article.)